

# Self-Adaptive Virtual Inertia Control-Based Fuzzy Logic to Improve Frequency Stability of Microgrid With High Renewable Penetration

著者	Kerdphol Thongchart, Watanabe Masayuki, Hongesombut Komsan, Mitani Yasunori
journal or publication title	IEEE Access
volume	7
page range	76071-76083
year	2019-06-05
URL	<a href="http://hdl.handle.net/10228/00007300">http://hdl.handle.net/10228/00007300</a>

doi: info:doi/10.1109/ACCESS.2019.2920886

Received April 4, 2019, accepted May 3, 2019, date of publication June 5, 2019, date of current version June 25, 2019.

Digital Object Identifier 10.1109/ACCESS.2019.2920886

# Self-Adaptive Virtual Inertia Control-Based Fuzzy Logic to Improve Frequency Stability of Microgrid With High Renewable Penetration

THONGCHART KERDPHOL<sup>1</sup>, (Member, IEEE), MASAYUKI WATANABE<sup>1</sup>, (Member, IEEE),  
KOMSAN HONGESOMBUT<sup>2</sup>, (Member, IEEE), AND YASUNORI MITANI<sup>1</sup>, (Member, IEEE)

<sup>1</sup>Department of Electrical and Electronic Engineering, Kyushu Institute of Technology, Kitakyushu, Fukuoka 804-8550, Japan

<sup>2</sup>Department of Electrical Engineering, Kasetsart University, Bangkok 10900, Thailand

Corresponding author: Thongchart Kerdphol (kerdphol@ele.kyutech.ac.jp)

This work was supported by the Power System and Renewable Energy Laboratory (Mitani-Watanabe Labs), Kyushu Institute of Technology, Kitakyushu, Fukuoka, Japan.

**ABSTRACT** Maintaining frequency stability of low inertia microgrids with high penetration of renewable energy sources (RESs) is a critical challenge. Solving this challenge, the inertia of microgrids would be enhanced by virtual inertia control-based energy storage systems. However, in such systems, the virtual inertia constant is fixed and selection of its value will significantly affect frequency stability of microgrids under different penetration levels of RESs. Higher frequency oscillations may occur due to the fixed virtual inertia constant or unsuitable selection of its value. To overcome such a problem and provide adaptive inertia control, this paper proposes a self-adaptive virtual inertia control system using fuzzy logic for ensuring stable frequency stabilization, which is required for successful microgrid operation in the presence of high RESs penetration. In this concept, the virtual inertia constant is automatically adjusted based on input signals of real power injection of RESs and system frequency deviations, avoiding unsuitable selection and delivering rapid inertia response. To verify the efficiency of the proposed control method, the contrastive simulation results are compared with the conventional method for serious load disturbances and various rates of RESs penetration. The proposed control method shows remarkable performance in transient response improvement and fast damping of oscillations, preserving robustness of operation.

**INDEX TERMS** Frequency control, fuzzy logic, intelligent control, islanded microgrid, virtual inertia control, virtual synchronous generator

## I. INTRODUCTION

Concerning on the environmental issue, energy shortage, and rapid economic growth, utilization of power electronic-based renewable energy sources (RESs) is gaining more attention for generating electrical power. Microgrids can offer a sufficient infrastructure for integrating RESs to the utility grid [1], [2]. Consequently, power electronic-based RESs have become the major components in existing microgrids. However, the dynamic stability (e.g., frequency/voltage control) and control/protection strategies must remain the priority. Currently, the high-level integration of RESs has created serious challenges including difficulties in maintaining frequency stability owing to the reduction in system

inertia triggered by the introduction of power electronic-based RESs [3]. Therefore, introducing RESs into microgrids significantly decreases the inertia of the whole system and the system voltage/frequency can be oscillated. Moreover, focusing on microgrid operation, microgrids may operate either in islanded or grid-connected modes. In the islanded mode, microgrids are more sensitive to encounter with challenges in voltage and frequency control. Especially, these issues would be worsen in case of the islanded microgrids with a high level of power electronic-based RESs due to the significant lack in system inertia. Accordingly, in the low inertia microgrids, power unbalances can cause rapid and severe changes in voltage and frequency oscillations, leading to the degradation of microgrid resiliency and stability [4].

To overcome these stability issues driven by the low system inertia, novel concepts of virtual inertia control

The associate editor coordinating the review of this manuscript and approving it for publication was Feiqi Deng.

(e.g., virtual synchronous machine and synthetic inertia) have been introduced [5]–[7]. The virtual inertia is imitated by high-level control of power inverters-based energy storage systems, increasing the whole system inertia and frequency performance/ stability [8]. The virtual inertia control systems addressed in [8]–[16] have been designed to connect ESS with the utility grid. It is guaranteed that the applications of virtual inertia control can efficiently supply uninterrupted power between the grid-connected and islanded modes for microgrid operation [9], [10]. In recent years, a virtual inertia control-based algebraic type was designed in [9] by a proportional gain and first order element, improving frequency stability of the microgrid. In [10], they proposed a control technique for inverters to imitate the characteristics of synchronous generators, increasing system inertia and damping. In [11], they presented a virtual inertia control method to improve dynamic performance of distributed/RESs generators. In [12], they implemented virtual inertia control-based supercapacitor to provide the inertia response of synchronous generators in an islanded microgrid. The effects of virtual inertia control on transient stability of a microgrid were investigated in [13]. In [7], they proposed virtual inertia emulation based on the rotor of doubly fed induction generator (DFIG) of wind turbines and supercapacitor. In [14], they applied an application of virtual inertia control to increase frequency performance of interconnected systems-based HVAC transmission line. In [15], they proposed a coordinated control between the virtual inertia control and HVDC system to enhance dynamic stability of interconnected systems. In [16], multiple HVDC interconnections have been controlled to contribute to the inertia of power systems.

While, in virtual inertia control-based above references, a virtual inertia constant value is fixed at one value for responding all penetration levels of RESs/disturbances. The selection of virtual inertia constant values in [8]–[16] is based on the trade-off or graphical analysis-based between the response time and dynamic performance of the system. Thus, it requires extensive eigenvalue sensitivity analysis, and may cause unsuitable selection or adjustment errors, leading to system instability. In addition to inertia constant, system frequency and power oscillate after the penetration of disturbances/RESs similar to those of synchronous generators, but the transient tolerance of power electronic-based RESs is much less than actual synchronous generators. Hence, using the fixed virtual inertia constant would significantly affect the frequency stability/performance of the system under different penetration levels of disturbances/RESs. Higher frequency oscillations after contingencies may occur due to the fixed virtual inertia constant or unsuitable selection of its value, deteriorating system stability, performance and resiliency.

To solve the stability problems caused by the fixed virtual inertia constant, the self-adaptive virtual inertia control techniques are proposed in [17]–[19]. In [17], they designed virtual inertia control with alternating moment of inertia to suppress power oscillations for microgrids. In [18], they proposed a self-tuning method of virtual inertia control to

improve frequency stability of a microgrid. In [19], they presented the adaptive virtual inertia control considering the effect of damping factor on frequency response. However, based on the aforementioned references, the proposed methods are complex to implement and the effect of high RESs penetration has not been considered for self-adaptive virtual inertia control. Moreover, with the increasing high renewable integration recently, the independent system operators (ISO) need new control techniques for existing and future microgrids [20]. These uncertainties and changes in high RESs integration can cause the self-adaptive inertia control methods to be unstable to provide a suitable performance over a wide range of microgrid operating conditions. Hence, without considering the effect of high RESs penetration in the control designs, the self-adaptive inertia control systems in [17]–[19] may be insufficient and unstable after high-level penetration of RESs, leading to higher frequency oscillations and system instability. In the worst case, the self-adaptive virtual inertia control may stop working owing to oscillations with high amplitude after high penetration of RESs, resulting in cascade outages and power blackouts. This is the major weakness of the aforementioned methods.

To deal with such a challenge and ensure stable/robust operation of a microgrid due to low system inertia created by high RESs penetration, this paper proposes the self-adaptive virtual inertia control-based fuzzy logic considering high RESs penetration. Since fuzzy logic control offers the simplicity, reliability and robustness including the advanced capability in solving non-linear problems, thus, the fuzzy logic has been applied in all fields of engineering and science including solving control issues in power system operation and control [20], [21]. In particular, the fuzzy logic can help in the modeling complex behavior of the system, where the direct correlation between the system input and output could not be evaluated through the equations by employing human understanding [22], [23]. In recent years, numerous studies have been reported for fuzzy logic-based numerous control/system configurations to improve frequency stability of power systems in [20] and [22]–[29]. However, no report focuses on the design and analysis of fuzzy logic-based virtual inertia control considering high RESs integration.

Therefore, this paper presents a novel intelligent methodology using the fuzzy logic control technique to enhance frequency performance of the low inertia microgrid under the situations of high RESs penetration. The higher-level application of virtual inertia control is created based on the derivative control method. The proposed fuzzy system utilizes the signals of system frequency deviations and real power changes of RESs to determine a simple fuzzy logic-based virtual inertia constant, enabling self-adaptive inertia response from the virtual inertia control system. The proposed control method offers the main contributions for existing and future microgrids owing to emerging high RESs integration, which the conventional virtual inertia control systems might not be appropriate to deliver the desired stability/performance over a wide range of microgrid operation. To verify the efficiency

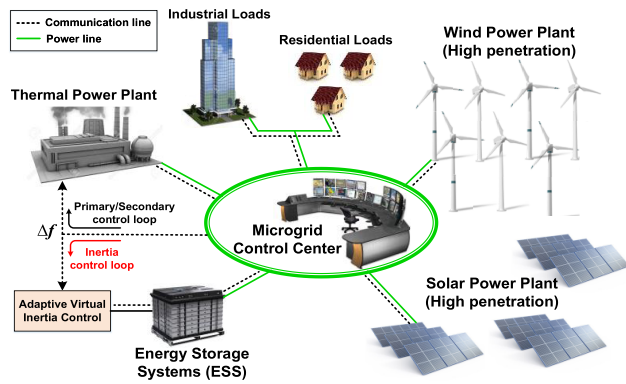


FIGURE 1. The simplified model of the studied microgrid.

of the proposed self-adaptive virtual inertia control technique, a computer simulation is conducted for modeling the microgrid test system, including high penetration of wind/solar farms, industrial and residential loads in MATLAB/Simulink software. The obtained results are compared with the conservative virtual inertia control design-based derivative control technique in [14]–[16] and [30].

After introduction, the rest of this paper is organized as follows: Section II introduces the dynamic structures of the studied microgrid, highlighting virtual inertia control and frequency response. Section III proposes the self-adaptive virtual inertia control-based fuzzy logic. Section IV displays the simulation results of the proposed control technique. Lastly, it summarizes with the main conclusions in Section V.

## II. SYSTEM CONFIGURATION

### A. MODELING OF THE STUDIED MICROGRID

The studied microgrid with RESs penetration employed in this work is shown in Fig. 1. The system consists of 12 MW of a non-reheat thermal power plant, 7 MW of a wind power plant, 4 MW of an energy storage system (ESS), 6 MW of a solar power plant, 10 MW of industrial loads, and 5 MW of residential loads. The 15 MW is used as the system base [31]. The communication links (i.e., dotted line) are used to connect the magnitude of electric devices in distributed locations, exchanging control instructions and status information. This study also assumed that the microgrid is not connected to any large power utility, operating as the stand-alone/islanded system [32].

To analysis frequency control, the dynamic model of the studied microgrid in the presence of RESs penetration is constructed in Fig. 2. This figure describes the block diagram of a typical microgrid control area with a conventional generation unit (i.e., thermal power plant) and renewable generation units (i.e., wind/solar power plants). To make the system close to practical conditions of the actual microgrid, this work applied the generator rate constraint (GRC) and the rate limitation of turbine-valve/gate closing or opening speed ( $V_U$ ,  $V_L$ ) for the conventional generator, creating system non-linearity [33], [34]. The GRC is considered as 12% p.u. MW/minute for non-reheat thermal power generation.

TABLE 1. Dynamic/control parameters of the microgrid.

Parameter	Value
Frequency bias factor, $\beta$ (p.u.MW/Hz)	1
Secondary frequency controller, $K_i$ (s)	0.05
Time constant of governor, $T_g$ (s)	0.1
Time constant of turbine, $T_t$ (s)	0.4
Droop characteristic, $R$ (Hz/p.u.MW)	2.4
System damping coefficient, $D$ (p.u.MW/Hz)	0.015
System inertia, $H$ (p.u.MW s)	0.083
Time constant of virtual inertia, $T_{VI}$ (s)	10
Time constant of wind turbine, $T_{WT}$ (s)	1.5
Time constant of solar system, $T_{PV}$ (s)	1.85
Maximum limit of valve gate speed, $V_U$	0.5
Minimum limit of valve gate speed, $V_L$	-0.5
Maximum capacity of ESS, $P_{inertia\ max}$	0.25
Minimum capacity of ESS, $P_{inertia\ min}$	-0.25

The thermal power station delivers the needed power, and offers primary frequency control to the microgrid. The area control error (ACE) is used to reduce the error of steady-state frequency for secondary frequency control. In addition to older/small power systems, the ACE may be neglected, where linearized models are used. The ESS helps the thermal power station in providing the needed power, and emulates inertia and damping characteristics for inertia control. The renewable power plants (i.e., wind/solar) can provide a considerable amount of power to the system, but these power plants are not participated in the frequency control. Thus, wind/solar power and load demand (i.e., residential and industrial loads) are assigned as the disturbances to the microgrid. Based on [15], [16] and [29]–[35], it is guaranteed that the dynamic model-based low-order used in Fig. 2 is accurate enough for frequency stability study and analysis. The microgrid/control parameters are defined in Table 1 [33].

### B. MODELING OF VIRTUAL INERTIA CONTROL

Replacing a number of conventional synchronous generation with a high level of RESs into microgrids introduces serious frequency stability problems owing to the lack in system inertia [3], [7]. For this reason, the concept of virtual inertia emulation/control is applied to generate the damping and inertia characteristics based on conventional synchronous generation, increasing system inertia/stability and allowing the RESs penetration in frequency control. In this study, it is presumed that the inertia power could be emulated using the combination of the ESS, power converter and control technique. Thus, the ESS is essentially an inertial unit, which can adjust the active power of the system, and regulate system frequency through inertia response by changing the control characteristic of the corresponding power converter.

To create the inertia power using the ESS, the dynamic structure of virtual inertia control is designed as shown in Fig. 3. In this study, the derivative control technique is the key concept of inertia control, which is able to determine the rate of change of frequency (ROCOF) to modify the extra active power to the set-point value of the system after the disturbance/RES penetration. To obtain the real behavior of the ESS, the low pass filter is added to the system,

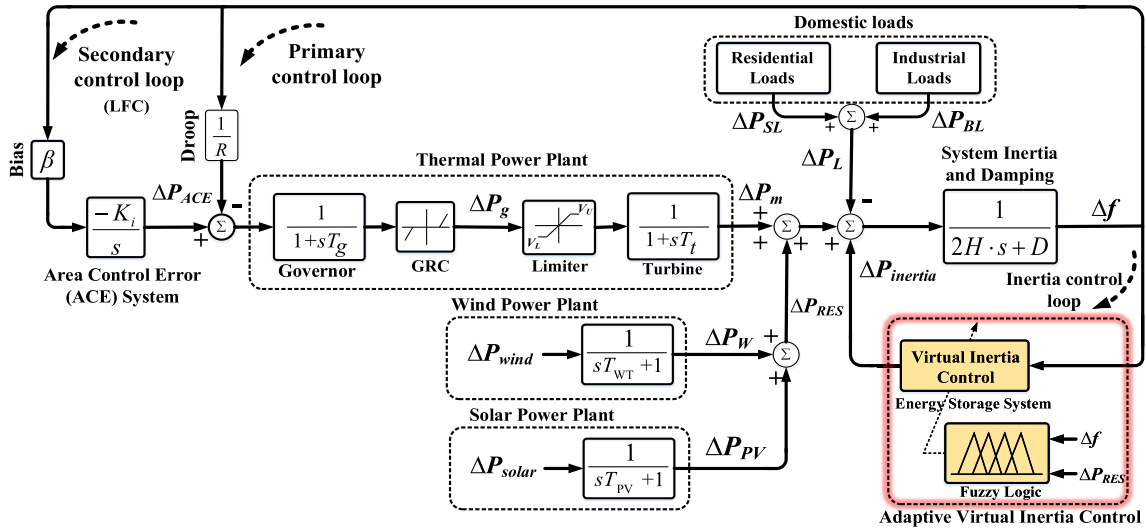


FIGURE 2. The dynamic model of the studied microgrid.

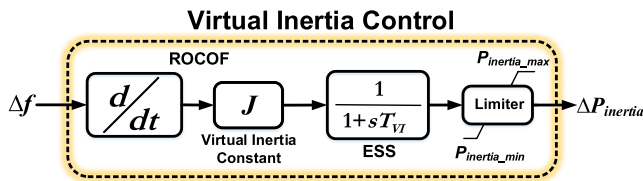


FIGURE 3. The dynamic model of virtual inertia control.

providing dynamic response. The filter-based low-pass type could also eliminate the noise problem caused by frequency measurements, since the derivative control is very sensitive to the noise. The limiter block is applied to restrict the minimum/maximum power capacity of the ESS, representing the practical energy condition of the ESS. Therefore, the dynamic model in Fig. 3 can virtually emulate the desired inertia power and characteristic to the studied microgrid during the disturbance/RESs penetration, increasing the whole system inertia, frequency performance and stability.

The dynamic equation for imitating virtual inertia power is evaluated using (1). During frequency deviations caused by the disturbance/RES penetration, if the active power via the power converter-based ESS is proportionally controlled by the ROCOF, the inertia power can be virtually emulated to the system, increasing inertia response of the microgrid as [15], [16] and [30]:

$$\Delta P_{inertia} = \frac{J}{1 + sT_{VI}} \left( \frac{d(\Delta f)}{dt} \right) \quad (1)$$

where  $J$  means the virtual inertia constant,  $T_{VI}$  means the virtual inertia time constant of the added filter for imitating the dynamic behavior of the ESS, and  $\Delta f$  means the system frequency deviation.

### C. FREQUENCY CONTROL FOR THE STUDIED MICROGRID

To preserve desirable stability and performance of the microgrid during high penetration of RESs, three main control

processes (i.e., primary control, secondary control and inertia control) are used in this study as follows:

- During inertia control, the processes of primary and secondary control have not been activated, thus, the system frequency is stabilized using the kinetic energy from the conventional generator or virtual inertia control-based ESS after the disturbance [15], [16], [30].
- During primary control, the system frequency is stabilized using the conventional generator to a new steady-state condition after the disturbance [33].
- During secondary control, the system frequency is recovered using the ACE to its nominal equilibrium state after the disturbance [33], [36].

To understand what inertia control is, this work describes the dynamic structure of frequency control focusing on inertia response. In conventional power systems, the dynamic behavior of synchronous generators based on the swing equation can be expressed as [35]:

$$J_s \frac{d\omega}{dt} = T_m - T_e = \frac{P_m}{\omega} - \frac{P_e}{\omega} \quad (2)$$

where  $J_s$  means the moment of inertia,  $\omega$  means the angular velocity of the synchronous rotor,  $T_m$  and  $T_e$  mean the mechanical and electrical torque for the generator,  $P_m$  and  $P_e$  mean the mechanical and electrical power for the generator.

The inertia power response is usually generated using the stored kinetic energy in synchronous generators. Thus, the kinetic energy ( $E_{kinetic}$ ) of system rotating mass including spinning loads is formed as [35]:

$$E_{kinetic} = \frac{1}{2} J_s \omega^2 \quad (3)$$

Since the dynamics of system frequency consist of the aggregated rotating/spinning dynamics, the system inertia ( $H$ ) can be defined as a proportion of kinetic energy and system power rating as [35]:

$$H = \frac{E_{kinetic}}{S} \quad (4)$$

where  $S$  is the system power rating-based synchronous machine.

Thus, the initial response to frequency deviations after the disturbance is stabilized by the system inertia ( $H$ ). The ROCOF means the time derivative of the frequency signal, which is used to calculate the inertia response of the system as [35], [37] and [38]:

$$ROCOF = \frac{d(\Delta f)}{dt} = \frac{f_0(P_m - P_e)}{2HS} \quad (5)$$

where  $f_0$  is the nominal system frequency.

Hence, the ROCOF is one of the important measurements, which the inertia control depends on. Afterwards, focusing on the dynamics of the studied microgrid, the control equations of each component (See Figs. 2 and 3) are formulated as follows:

$$\Delta P_m = \frac{1}{1 + sT_i} (\Delta P_g) \quad (6)$$

$$\Delta P_g = \frac{1}{1 + sT_g} \left( \Delta P_{ACE} - \frac{1}{R} \Delta f \right) \quad (7)$$

$$\Delta P_{ACE} = \frac{K_i}{s} (\beta \cdot \Delta f) \quad (8)$$

$$\Delta P_{RES} = \Delta P_W + \Delta P_{PV} \quad (9)$$

$$\Delta P_W = \frac{1}{1 + sT_{WT}} (\Delta P_{wind}) \quad (10)$$

$$\Delta P_{PV} = \frac{1}{1 + sT_{PV}} (\Delta P_{solar}) \quad (11)$$

$$\Delta P_L = \Delta P_{SL} + \Delta P_{BL} \quad (12)$$

Therefore, the control law/dynamic equation for frequency deviations in the studied microgrid considering the effects of inertia control, primary control and secondary control can be modified using (1) and (6) – (12) as:

$$\Delta f = \frac{1}{2HS + D} (\Delta P_m + \Delta P_{RES} + \Delta P_{inertia} - \Delta P_L) \quad (13)$$

where  $H$  is the equivalent microgrid inertia or system inertia,  $D$  is the equivalent microgrid damping coefficient,  $\Delta P_m$  is the generated power change from the thermal power plant,  $\Delta P_{RES}$  is the total generated power change from the renewable power plants,  $\Delta P_{inertia}$  is the virtual inertia power change from the ESS,  $\Delta P_L$  is the total load change of the system,  $\Delta P_g$  is the generated power change from the governor unit-based thermal power plant,  $\Delta P_{ACE}$  is the control signal change for secondary control,  $K_i$  is the supplementary frequency controller,  $\Delta P_W$  is the generated power change from the wind power plant,  $\Delta P_{wind}$  is the initial wind speed power change,  $\Delta P_{PV}$  is the generated power change from the solar power plant,  $\Delta P_{solar}$  is the initial solar radiation power change,  $\Delta P_{SL}$  is the load power change from the residential area and  $\Delta P_{BL}$  is the load power change from the industrial area.

### III. SELF-ADAPTIVE VIRTUAL INERTIA CONTROL BASED FUZZY LOGIC

Fuzzy logic is a heuristic supervised learning methodology, which utilizes the human understanding or knowledge of

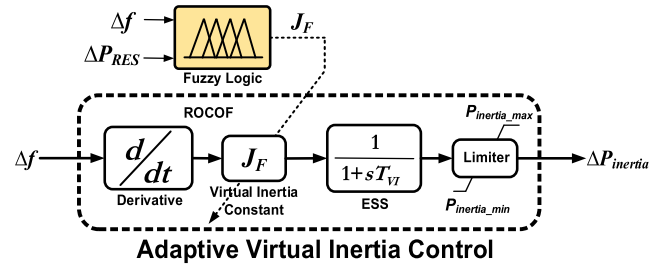


FIGURE 4. The schematic of the proposed self-adaptive virtual inertia control.

experts/operators to establish the control system. Due to its simplicity, reliability and robustness, fuzzy logic has been implemented in all fields of engineering and science, including solving control problems [20], [21]. In power system operation and control, fuzzy logic can handle problems with the capability in solving system uncertainty and non-linear or un-modeled systems [28]. In addition to system modeling, it helps in modeling complex behavior, where the direct correlation between the system input and output cannot be evaluated by equations. In decades, the fuzzy logic has been widely implemented to adjust the controller gains. After the change of system operation, the gains of controllers are tuned using the fuzzy system based on a set of “if-then” rules [22], [24].

In recent years, virtual inertia control techniques with a fixed virtual inertia constant or control gain are widely used to emulate the inertia and damping characteristics of synchronous generators, increasing system inertia and responding all penetration levels of disturbances/RESs [14]–[16], [30]. The control signal of conventional virtual inertia control with a fixed virtual inertia constant is defined as (1). However, the conventional virtual inertia control cannot provide the reasonable performance under different penetration levels of disturbances/RESs due to the fixed virtual inertia constant.

In this study, the fuzzy system is utilized to adapt the virtual inertia constant of virtual inertia control, enabling self-adaptive and fast inertia response to the microgrid. The schematic of the proposed self-adaptive virtual inertia control can be demonstrated in Fig. 4. During frequency deviations with low RESs penetration, if the microgrid is operated with a big value of virtual inertia constant, it can cause longer settling time in stabilizing the system frequency, leading to slow damping of oscillations. In such a situation, the system would need a small value of virtual inertia constant to deal with the system frequency, delivering fast damping of oscillations. On the contrary, during frequency deviations with high RESs penetration, a big value of virtual inertia constant is significantly required to reduce the oscillations with high amplitude caused by high RESs penetration corresponding to low system inertia, avoiding system instability and collapses. Thus, if the virtual inertia control system can properly adjust the virtual inertia constant to track the changes in disturbances/RESs penetration, the optimal performance and stability of the microgrid can be achieved. To calculate the

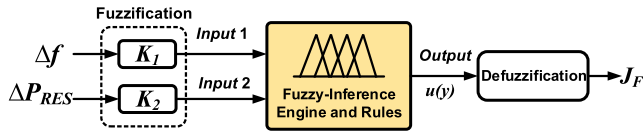


FIGURE 5. The structure of the fuzzy system-based self-adaptive virtual inertia constant.

appropriate value of virtual inertia constant and enable self-adaptive virtual inertia control, the proposed fuzzy system is utilized by combining the fuzzy interface with fuzzy rules. From (1), the virtual inertia constant will be automatically adjusted by the knowledge base and fuzzy interface of real power changes of RESs and system frequency deviations.

The proposed fuzzy system consists of the fuzzification, inference engine, fuzzy rule base, and defuzzification, as displayed in Fig. 5. The real power changes of RESs ( $\Delta P_{RES}$ ) and system frequency deviations ( $\Delta f$ ) are used for inputs of the fuzzy system. The output is a normalized value of the virtual inertia constant ( $J_F$ ). There are two inputs and one output for the fuzzy system. Initially, the fuzzification is used to convert the actual inputs to the fuzzy values. Thus, *Input 1* and *Input 2* can be formed as:

$$Input\ 1 = \Delta f \cdot K_1 \tag{14}$$

$$Input\ 2 = \Delta P_{RES} \cdot K_2 \tag{15}$$

where  $K_1$  and  $K_2$  are scale factors of the fuzzification system. In this study,  $K_1 = K_2 = 1$ .

Later, the fuzzy values of *Input 1* and *Input 2* are forwarded to the fuzzy inference engine with the rule base. The fuzzy rule base is the fundamental operation of fuzzy logic for mapping the input signal to the output signal. To evaluate the suitable value of  $J_F$ , the fuzzy rule base is used by combining the input signals of  $\Delta P_{RES}$  and  $\Delta f$ . From Table 2, 15 fuzzy rules are determined based on the knowledge and practical experiences of the virtual inertia control and operation as follows:

1) When  $\Delta f$  and  $\Delta P_{RES}$  are relatively small, a zero value of  $J_F$  should be used to stabilize the system frequency, delivering fast damping of oscillations.

2) When  $\Delta f$  and  $\Delta P_{RES}$  are relatively large, a medium value (in case of negative large  $\Delta f$ ) or very big value (in case of positive large  $\Delta f$ ) of  $J_F$  should be used to reduce the oscillations with high amplitude caused by the high RESs and system inertia reduction, avoiding system instability and collapses.

3) When  $\Delta f$  is relatively small and  $\Delta P_{RES}$  is relatively large, a medium value (in case of negative small  $\Delta f$ ) or very big value (in case of positive small  $\Delta f$ ) of  $J_F$  should be applied to stabilize the system frequency with high amplitude caused by the high RESs and system inertia reduction, avoiding system instability and collapses.

4) When  $\Delta f$  is relatively large and  $\Delta P_{RES}$  is relatively small, a zero value (in case of negative large  $\Delta f$ ) or medium value (in case of positive large  $\Delta f$ ) of  $J_F$  should be used to

TABLE 2. Fuzzy rules of self-adaptive virtual inertia control for linguistic variable.

		$\Delta f$				
		NL	NS	ZO	PS	PL
$\Delta P_{RES}$	L	ZO	ZO	ZO	ZO	M
	M	S	S	M	B	B
	H	M	M	M	VB	VB

stabilize the system frequency, delivering fast damping with low frequency oscillations.

By utilizing Table 2, the fuzzy rules is defined in the form of “if-then” conditions as follows:

**If *Input 1* is *A* and *Input 2* is *B*, Then  $J_F$  is *C*.**

where *A*, *B*, and *C* mean the fuzzy set on the corresponding sets.

The various fuzzy rules and membership functions for the inputs and output of the fuzzy system are designed in Fig. 6 and Table 2. The *Input 1* has three triangular and two trapezoidal memberships, whereas the *Input 2* has one triangular and two trapezoidal memberships. The output of the fuzzy system has two trapezoidal and three triangular memberships. The triangular membership function is selected because it has the characteristics of remarkable control performance and simplified calculation [28]. The range of fuzzy variables used in this study are  $\Delta f = [-0.5, 0.5]$  Hz, and  $\Delta P_{RES} = [0, 1]$  p.u. The output range of  $J_F$  is set as  $[0, 4]$  s, which is optimally determined based on the extensive eigenvalue sensitivity analysis in [15] and [30].  $\mu$  means the grade of each membership. The inputs and output are divided into fuzzy subsets, and defined using linguistic variable. NL is negative large, NS is negative small, ZO is zero, PS is positive small, PL is positive large, L is low, M is medium, H is high, S is small, B is big, and VB is very big.

The fuzzy inference engine changes the fuzzy rules to the fuzzy linguistic output in Table 2. However, the fuzzy linguistic output is unavailable for the signal of equalization control. To solve such a problem, the defuzzification process is required. Finally, the results from the fuzzy rules are sent to the defuzzification, and converted to the crisp values using the centroid defuzzification method as [39]:

$$J_F = \frac{\sum_{i=1}^{Ru} y_i \cdot u(y_i)}{\sum_{i=1}^{Ru} u(y_i)} \tag{16}$$

where  $y_i$  means the value of the output, which corresponds to the grade  $\mu_i$  for the  $i^{th}$ .  $Ru$  means the number of fuzzy rules.

By utilizing the proposed fuzzy system, the virtual inertia constant can be automatically adjusted to track the changes in different penetration levels of disturbances/RESs, enabling self-adaptive inertia response. The dynamic equation of the self-adaptive virtual inertia control can be established as:

$$\Delta P_{inertia} = \frac{J_F}{1 + sT_{VI}} \left( \frac{d(\Delta f)}{dt} \right) \tag{17}$$

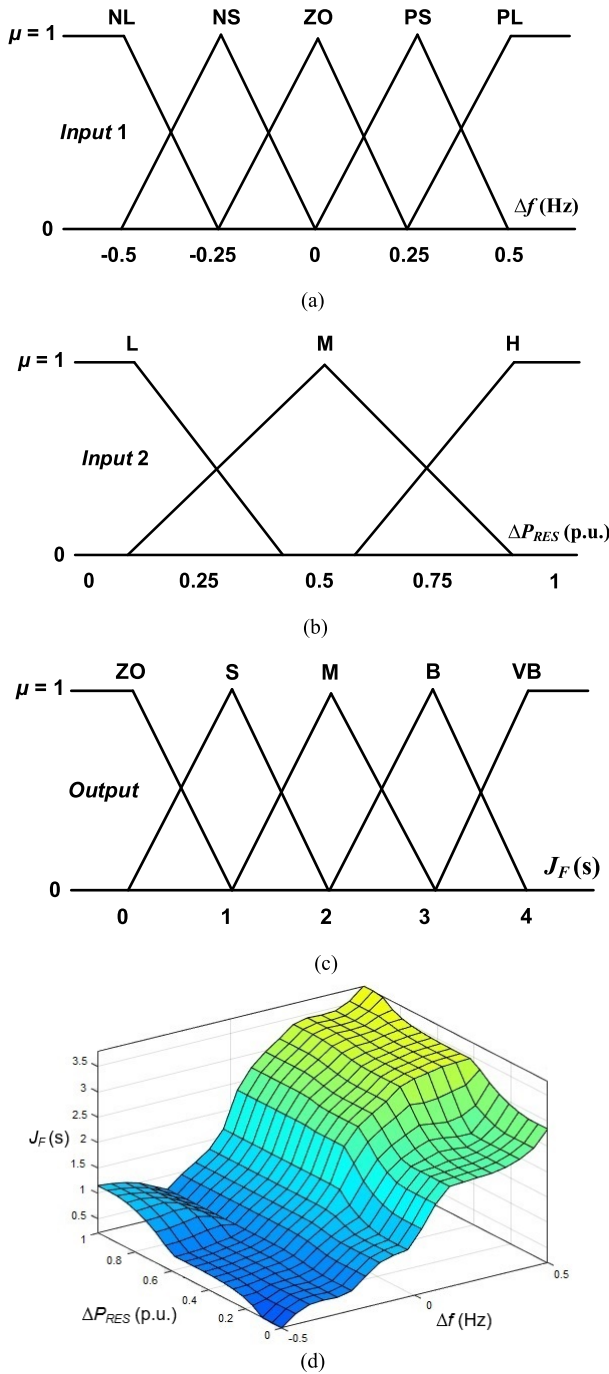


**FIGURE 6.** Symmetric fuzzy membership functions: (a) System frequency deviations. (b) RESs power changes/penetration. (c) Virtual inertia constant. (d) Effect of RESs penetration and system frequency deviations on the output of the fuzzy system.

Therefore, the proposed self-adaptive virtual inertia control is not only to provide fast damping with low frequency deviations and sufficient inertia response, but also to effectively reduce the high amplitude/overshoot of oscillations under different penetration levels of disturbances/RESs.

#### IV. SIMULATION RESULTS AND ANALYSIS

This section presents the necessity of employing the self-adaptive virtual inertia control-based fuzzy logic over the

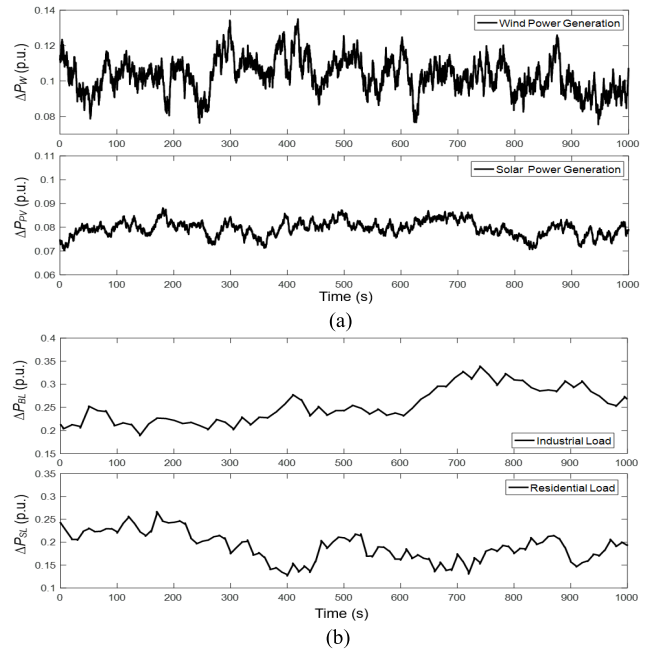


**FIGURE 7.** Multiple disturbances for scenario 1: (a) Renewable power generations under the situations of low wind velocity and solar radiation, (b) Industrial/residential load consumption patterns.

serious reduction of microgrid inertia driven by the increasing penetration of RESs. The impacts of the fuzzy logic contribution for the inertia control are also demonstrated. Since the higher-level application of virtual inertia control in this paper is created based on the derivative control technique, thus, the performance of the proposed control technique is compared with the conventional virtual inertia control-based derivative control technique in [14]–[16] and [30]. In addition to the conventional technique, the fixed virtual inertia constant ( $J = 0.85$ ) is properly obtained based on the extensive eigenvalue sensitivity and trade-off analysis. To demonstrate the efficiency and robustness of the proposed self-adaptive inertia control design, nonlinear simulations are carried out using MATLAB/Simulink software. Contrastive critical scenarios with different penetration rates of RESs, load patterns, system inertia, and control parameters are conducted for examining microgrid frequency response. According to the frequency operating standard for islanded systems used today [40], the acceptable limits of frequency deviations in this work are defined as 49.5 to 50.5 Hz ( $\pm 0.5$  Hz) during no contingency event, and as 49 to 51 Hz ( $\pm 1$  Hz) during the generation/load event.

#### A. SCENARIO 1: 20% OF RESs PENETRATION

For Scenario 1, the frequency response of the system is tested under a normal condition of high system inertia (i.e., 20% reduction from its nominal value). The microgrid operations are slightly disturbed by low power penetration of wind/solar farms, and industrial/residential load patterns as seen in Fig. 7.

From Fig. 8, the connection of 0.06 p.u. in the wind farm at  $t = 200$  s causes the frequency overshoots of 0.4 and 0.3 Hz



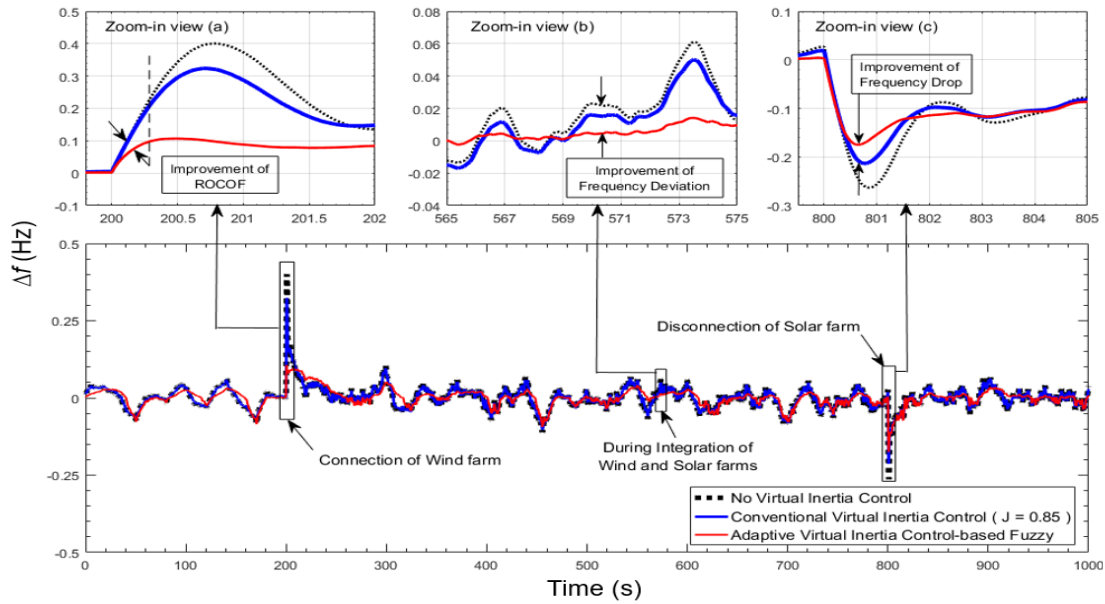


FIGURE 8. Microgrid frequency response during low RESs penetration corresponding to high system inertia (scenario 1).

in the cases of no virtual inertia control and conventional control. The frequency overshoot of the microgrid is significantly reduced in case of the proposed control technique due to the involvement of fuzzy logic-based self-adaptive inertia control. Obviously, the proposed control technique can significantly improve the performance of ROCOF, thus, the smaller frequency overshoot is obtained. During the penetration of wind and solar generations at  $t = 200 - 800$  s, the better performance for the proposed control technique can be observed in comparison of conventional control in deriving the system frequency deviation close to zero. The disconnection of 0.07 p.u. in the solar farm at  $t = 800$  s results in the sudden frequency drops of 0.26 and 0.21 Hz in the cases of no virtual inertia control and conventional control. Evidently, the system frequency drop is significantly enhanced owing to the proposed control technique, maintaining the stable frequency stability and performance of the microgrid.

Fig. 9(a) shows the suitable adaptation of virtual inertia constant during the normal microgrid operation. Compared with the conventional control, the self-adaptive virtual inertia control-based fuzzy could properly adjust the virtual inertia constant to track the changes in penetration levels of wind and solar generations, delivering faster response with smaller oscillations. Fig. 9(b) shows that the proposed control technique can extract more inertia power from the ESS by discharging than the conventional inertia control. Thus, the main generation-based thermal unit is less stressed, and requires less power generation due to the proposed control technique as shown in Fig. 10.

**B. SCENARIO 2: 80% OF RESs PENETRATION**

To conduct the severe test scenario, the total penetration of RESs is increased to 80% of its capacities (See Fig. 11) and the frequency response of the system is examined under the

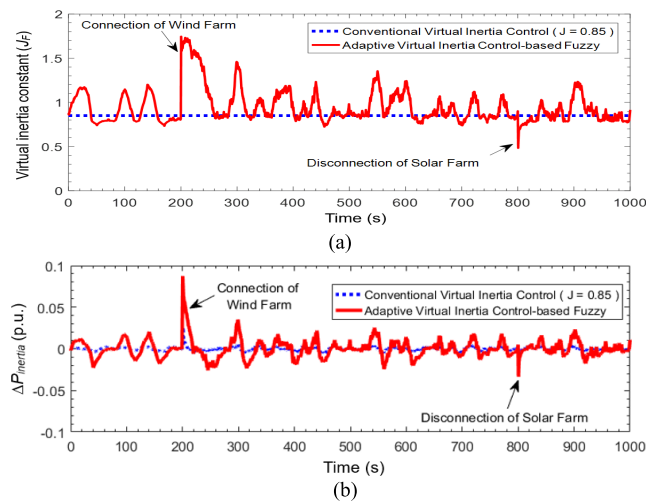


FIGURE 9. Virtual inertia response for Scenario 1: (a) Virtual inertia constant. (b) Virtual inertia power deviations.

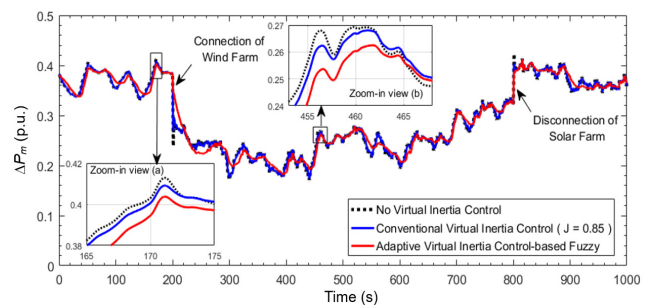
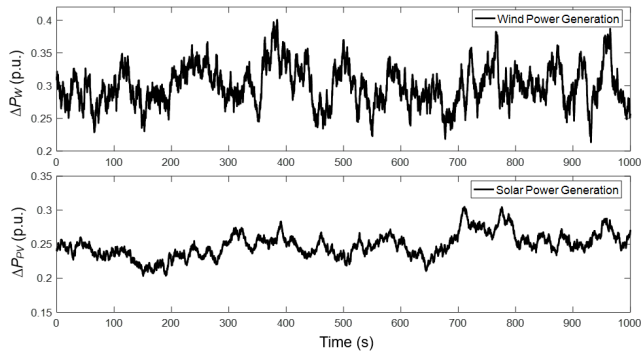
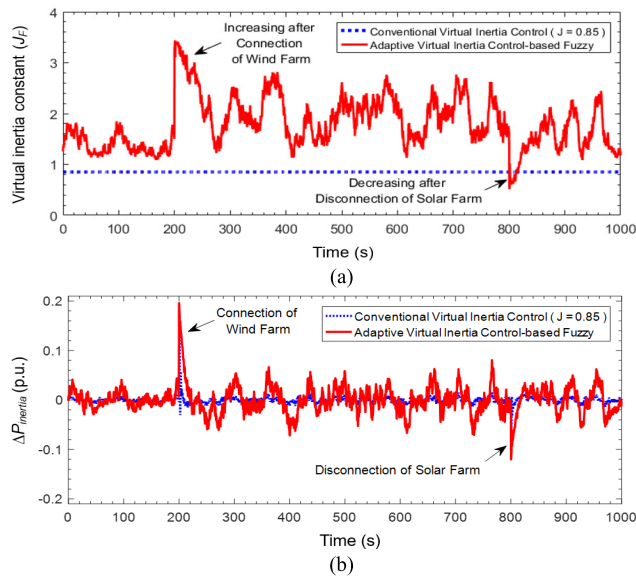


FIGURE 10. Thermal power response for scenario 1.

critical condition of low system inertia (i.e., 60% reduction from its nominal value). To represent more drastic operating conditions from the frequency stability point of view, the high



**FIGURE 11.** Renewable power generations under the situations of high wind velocity and solar radiation for scenarios 2 and 3.



**FIGURE 12.** Virtual inertia response for scenario 2: (a) Virtual inertia constant. (b) Virtual inertia power deviations.

power generations from wind/solar farms are connected to the system at the similar load demand patterns as shown in Fig. 7b, causing low load damping factor (i.e., higher frequency oscillations).

Following the serious event, the well-adjustment of virtual inertia constant during the high RESs penetration is shown in Fig. 12(a). Obviously, the adjustment rate of virtual inertia constant increases after the connection of wind energy, and decreases after the disconnection of solar energy due to the employment of fuzzy logic-based adaptive inertia control. Compared with the traditional control, the self-adaptive virtual inertia control-based fuzzy is able to track the severe changes in high penetration of RESs, leading to the fast damping of oscillations with low amplitude. Fig. 12(b) demonstrates that the virtual inertia power is greatly discharged using the proposed control technique, ensuring the robustness of system operation. Fig. 13 shows the main power generation from the thermal unit. In case of no inertia control, the thermal generation unit is unstable to maintain the required power generation due to high renewable integration and low system

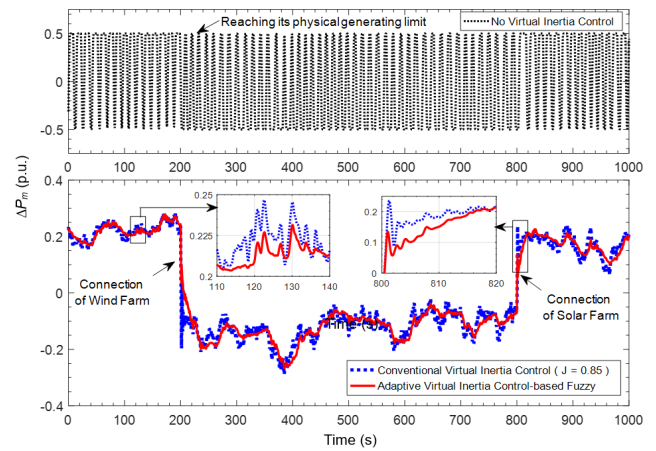


**FIGURE 13.** Thermal power response for scenario 2.

inertia, causing further cascade events. While, the proposed self-adaptive inertia control could effectively help the thermal unit in maintaining the required power generation with less oscillations compared with the conventional control, reducing the risk of reaching its physical limit and avoiding further cascade events.

As a result in Fig. 14, the system frequency is more fluctuated during this scenario. Without the inertia control, the system frequency severely fluctuates, ultimately leading to the instability and wide area power blackout. Using both the proposed adaptive and traditional inertia control, the system frequency can be alleviated. In case of the conventional control, the transition states during the connection of 0.34 p.u. in the wind farm and disconnection of 0.24 p.u. in the solar farm cause the large transients of about  $\pm 1.5$  Hz, which exceed the acceptable frequency standard limits, resulting in unstable conditions of the microgrid. Conversely, it is evident that the proposed technique provides the more stabilizing effect during high renewable integration and low system inertia. Consequently, the system frequency can be maintained in the permissible limits, implying the robustness of microgrid operation.

### C. SCENARIO 3: MISMATCH PARAMETERS OF PRIMARY AND SECONDARY CONTROL

In practical microgrids, it is possible to have an inaccuracy of parameters estimated for designing the system. Besides, the system parameters might vary by time, seriously deteriorating the system performance and causing the system instability. Therefore, it is necessary to investigate the microgrid stability and performance under the system parameter variations including primary and secondary control. In this scenario, both the proposed self-adaptive inertia control and conventional inertia control are responsible for providing primary frequency support during the mismatch microgrid control parameters. To demonstrate the adaptive property and robustness of the proposed control technique-based fuzzy logic, this test scenario is applied the severe disturbances similar to Scenario 2, but the system parameters including

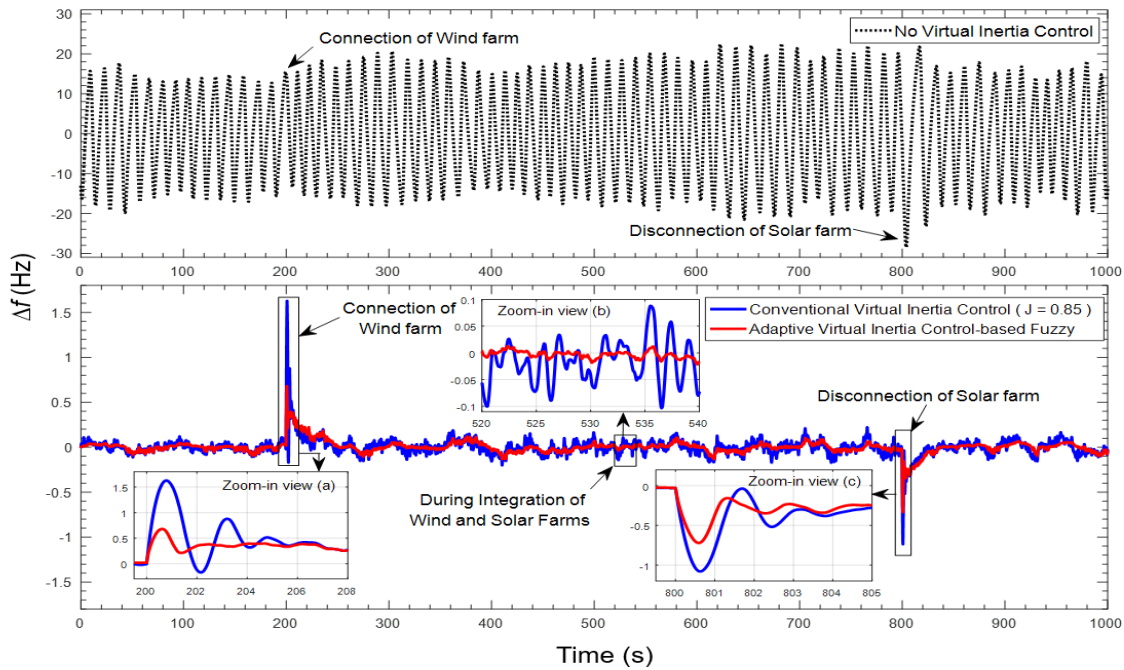


FIGURE 14. Microgrid frequency response during high RESs penetration corresponding to low system inertia (Scenario 2).

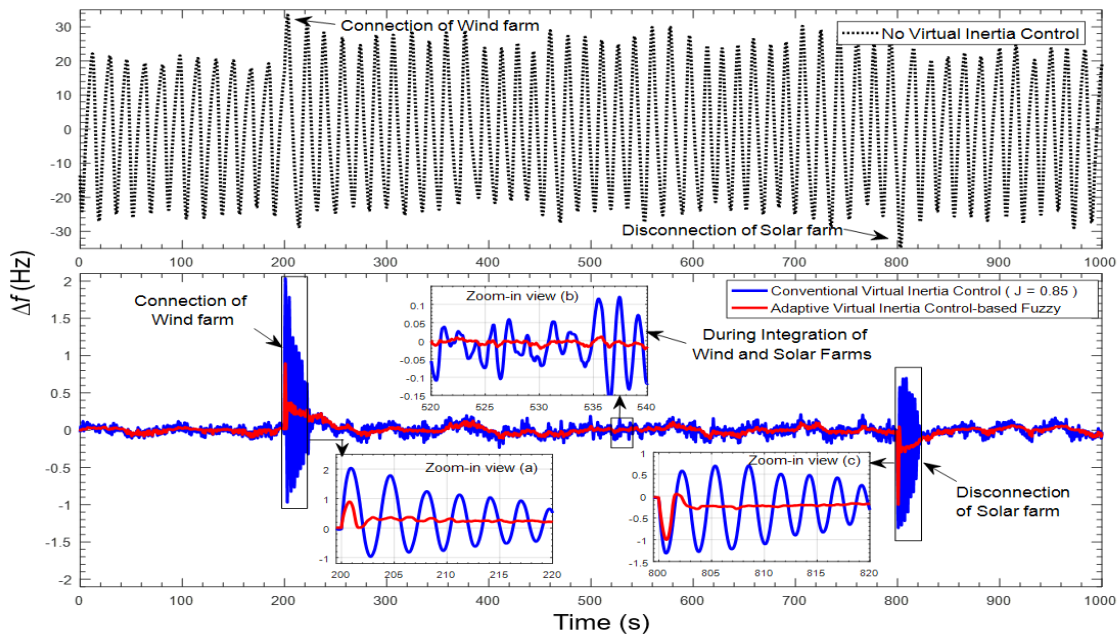


FIGURE 15. Microgrid frequency response during the mismatch primary/secondary control and microgrid parameters (Scenario 3).

primary and secondary control are drastically changed due to Table 3.

It can be seen from Fig. 15 that serious frequency deviations can be clearly observed. Without the virtual inertia control, it becomes impossible to maintain the system frequency stability, creating cascade failures and widespread black-outs. During the transitions of wind and solar generations at

$t = 200$  s and  $t = 800$  s, the conventional virtual inertia control with the fixed inertia constant cannot handle the applied parameter perturbation, causing larger frequency oscillations and overshoots of about  $\pm 2$  Hz with longer settling time of about 20 s (implying slow damping of oscillations). It shows that the conventional inertia control is not robust enough to a wide range of disturbances,

**TABLE 3. Microgrid uncertainty parameters and variation range (%) for each scenario.**

Uncertainty parameter	Nominal value	Scenario 1	Scenario 2	Scenario 3
Droop characteristic ( $R$ )	2.4	2.4	2.4	1.8 (-25%)
Time constant of governor ( $T_g$ )	0.1	0.1	0.1	0.15 (+50%)
Time constant of turbine ( $T_t$ )	0.4	0.4	0.4	0.7 (+75%)
Frequency bias factor ( $\beta$ )	1	1	1	0.8 (-20%)
Secondary controller ( $K_i$ )	0.05	0.05	0.05	0.04 (-20%)
System damping coefficient ( $D$ )	0.015	0.015	0.015	0.0135 (-10%)
System inertia ( $H$ )	0.083	0.067 (-20%)	0.032 (-60%)	0.025 (-70%)

**TABLE 4. Calculated performance index of microgrid frequency deviations.**

Scenario	Mean absolute frequency deviation (Hz)		
	No virtual inertia control	Conventional virtual inertia control	Self-adaptive virtual inertia control-based fuzzy logic
1	0.03504	0.03351	0.03167
2	10.4938	0.06129	0.05981
3	14.7835	0.08473	0.06863

significantly affecting the stable microgrid operation. However, the proposed control technique can increase the damping performance of the microgrid, thus, the frequency oscillations are smaller than the conventional one. Consequently, the system frequency is properly maintained within the acceptable frequency standard limits. This scenario implies that the self-adaptive virtual inertia control-based fuzzy logic is very robust against a wide range of microgrid operations including parameter variations, preserving the stable frequency stability even in more drastic conditions.

From Table 4, the performance index of the microgrid frequency deviation is evaluated for all test scenarios. It is obvious that the evaluation indices are quite better when the self-adaptive virtual inertia control-based fuzzy logic is applied, ensuring stable frequency stabilization.

## V. CONCLUSION

The significant issue raised in the existing and future microgrids is the frequency control under the situation of low system inertia due to high renewable integration. In this paper, enhancing the frequency stability of low inertia microgrid under high RESs penetration and serious disturbances is investigated. It has been shown that the conventional virtual inertia control technique with a fixed virtual inertia constant provided a poor performance, and could not guarantee the frequency stability of low inertia microgrid under the different penetration levels of RESs/disturbances. In response to this challenge, the self-adaptive virtual inertia control-based fuzzy logic has been proposed in this paper to track the changes in different levels of RESs/disturbances, enhancing frequency stability of low inertia microgrid. The proposed fuzzy logic-based virtual inertia control adopts the suitable value of virtual inertia constant considering real power changes of RESs and frequency deviations of the microgrid. By applying a big value of virtual inertia constant during high RESs penetration, the frequency transients and oscillations are significantly reduced. On the contrary, a small

value of virtual inertia constant is adapted during low RESs penetration, increasing the performance of fast damping of oscillations. The simulation results confirm that the stabilizing performance and robustness of the microgrid frequency stability with the proposed control technique are superior to the conventional control against various penetration levels of disturbances and RESs penetration. Besides, this paper shows the importance of the proposed fuzzy logic in making the self-adaptive virtual inertia response dynamically to RESs/disturbance changes during the drastic situation of low inertia microgrid.

## REFERENCES

- [1] T. John and S. P. Lam, "Voltage and frequency control during microgrid islanding in a multi-area multi-microgrid system," *IET Gener., Transmiss. Distrib.*, vol. 11, no. 6, pp. 1502–1512, 2017.
- [2] K. S. Rajesh, S. S. Dash, R. Rajagopal, and R. Sridhar, "A review on control of ac microgrid," *Renew. Sustain. Energy Rev.*, vol. 71, no. 1, pp. 814–819, 2017.
- [3] D. E. Olivares, "Trends in microgrid control," *IEEE Trans. Smart Grid*, vol. 5, no. 4, pp. 1905–1919, Jul. 2014.
- [4] F. M. Uriarte, C. Smith, S. Van Broekhoven, and R. E. Hebner, "Microgrid ramp rates and the inertial stability margin," *IEEE Trans. Power Syst.*, vol. 30, no. 6, pp. 3209–3216, Nov. 2015.
- [5] H.-P. Beck and R. Hesse, "Virtual Synchronous Machine," in *Proc. 9th Int. Conf. Elect. Power Qual. Utilisation (EPQU)*, 2007, pp. 1–6.
- [6] J. Driesen and K. Visscher, "Virtual synchronous generators," in *Proc. IEEE Power Energy Soc. Gen. Meeting, Convers. Del. Elect. Energy 21st Century (PES)*, Jul. 2008, pp. 1–3.
- [7] M. F. M. Arani and E. F. El-Saadany, "Implementing virtual inertia in DFIG-based wind power generation," *IEEE Trans. Power Syst.*, vol. 28, no. 2, pp. 1373–1384, May 2013.
- [8] H. Bevrani, T. Ise, and Y. Miura, "Virtual synchronous generators: A survey and new perspectives," *Int. J. Electr. Power Energy Syst.*, vol. 54, pp. 244–254, Jan. 2014.
- [9] Y. Hirase, K. Abe, K. Sugimoto, and Y. Shindo, "A grid-connected inverter with virtual synchronous generator model of algebraic type," *Elect. Eng. Jpn.*, vol. 184, no. 4, pp. 10–21, 2013.
- [10] S. D'Arco, J. A. Suul, and O. B. Fosso, "A virtual synchronous machine implementation for distributed control of power converters in SmartGrids," *Electr. Power Syst. Res.*, vol. 122, no. 1, pp. 180–197, 2015.
- [11] T. Shintai, Y. Miura, and T. Ise, "Oscillation damping of a distributed generator using a virtual synchronous generator," *IEEE Trans. Power Del.*, vol. 29, no. 2, pp. 668–676, Apr. 2014.

- [12] L. Sigrist, I. Egado, E. L. Miguélez, and L. Rouco, "Sizing and controller setting of ultracapacitors for frequency stability enhancement of small isolated power systems," *IEEE Trans. Power Syst.*, vol. 30, no. 4, pp. 2130–2138, Jul. 2015.
- [13] N. Soni, S. Doolla, and M. C. Chandorkar, "Improvement of transient response in microgrids using virtual inertia," *IEEE Trans. Power Del.*, vol. 28, no. 3, pp. 1830–1838, Jul. 2013.
- [14] T. Kerdpol, F. S. Rahman, and Y. Mitani, "Virtual inertia control application to enhance frequency stability of interconnected power systems with high renewable energy penetration," *Energies*, vol. 11, no. 4, pp. 981–997, 2018.
- [15] E. Rakhshani, D. Remon, A. M. Cantarellas, and P. Rodriguez, "Analysis of derivative control based virtual inertia in multi-area high-voltage direct current interconnected power systems," *IET Gener. Transmiss. Distrib.*, vol. 10, no. 6, pp. 1458–1469, Apr. 2016.
- [16] E. Rakhshani, D. Remon, A. M. Cantarellas, J. M. Garcia, and P. Rodriguez, "Virtual synchronous power strategy for multiple HVDC interconnections of multi-area AGC power systems," *IEEE Trans. Power Syst.*, vol. 32, no. 3, pp. 1665–1677, May 2017.
- [17] J. Alipoor, Y. Miura, and T. Ise, "Power system stabilization using virtual synchronous generator with alternating moment of inertia," *IEEE J. Emerg. Sel. Topics Power Electron.*, vol. 3, no. 2, pp. 451–458, Jun. 2015.
- [18] M. A. Torres, L. A. C. Lopes, L. A. T. Moran, and J. R. C. Espinoza, "Self-tuning virtual synchronous machine: A control strategy for energy storage systems to support dynamic frequency control," *IEEE Trans. Energy Convers.*, vol. 29, no. 4, pp. 833–840, Dec. 2014.
- [19] D. Li, Q. Zhu, S. Lin, and X. Y. Bian, "A self-adaptive inertia and damping combination control of VSG to support frequency stability," *IEEE Trans. Energy Convers.*, vol. 32, no. 1, pp. 397–398, Mar. 2017.
- [20] S. Zhang, Y. Mishra, and M. Shahidehpour, "Fuzzy-logic based frequency controller for wind farms augmented with energy storage systems," *IEEE Trans. Power Syst.*, vol. 31, no. 2, pp. 1595–1603, Mar. 2016.
- [21] C. Bhattacharjee and B. K. Roy, "Fuzzy-supervisory control of a hybrid system to improve contractual grid support with fuzzy proportional-derivative and integral control for power quality improvement," *IET Gener. Transmiss. Distrib.*, vol. 12, no. 7, pp. 1455–1465, 2017.
- [22] J. Talaq and F. Al-Basri, "Adaptive fuzzy gain scheduling for load frequency control," *IEEE Trans. Power Syst.*, vol. 14, no. 1, pp. 145–150, Feb. 1999.
- [23] A. Feliachi and D. Rerkpreedapong, "NERC compliant load frequency control design using fuzzy rules," *Electr. Power Syst. Res.*, vol. 73, no. 2, pp. 101–106, 2005.
- [24] C.-F. Juang and C.-F. Lu, "Load-frequency control by hybrid evolutionary fuzzy PI controller," *IEE Proc.-Gener. Transmiss. Distrib.*, vol. 153, no. 2, pp. 196–204, 2006.
- [25] P. Subbaraj and K. Manickavasagam, "Automatic generation control of multi-area power system using fuzzy logic controller," *Eur. Trans. Elect. Power*, vol. 18, no. 3, pp. 266–280, 2008.
- [26] C. S. Rao, S. S. Nagaraju, and P. S. Raju, "Automatic generation control of TCPS based hydrothermal system under open market scenario: A fuzzy logic approach," *Int. J. Elect. Power Energy Syst.*, vol. 31, no. 7, pp. 315–322, 2009.
- [27] T. Chaiyatham and I. Ngamroo, "Improvement of power system transient stability by PV farm with fuzzy gain scheduling of PID controller," *IEEE Syst. J.*, vol. 11, no. 3, pp. 1684–1691, Sep. 2017.
- [28] H. Bevrani and P. R. Daneshmand, "Fuzzy logic-based load-frequency control concerning high penetration of wind turbines," *IEEE Syst. J.*, vol. 6, no. 1, pp. 173–180, Mar. 2012.
- [29] M. Datta and T. Senjyu, "Fuzzy control of distributed PV inverters/energy storage systems/electric vehicles for frequency regulation in a large power system," *IEEE Trans. Smart Grid*, vol. 4, no. 1, pp. 479–488, Mar. 2013.
- [30] E. Rakhshani and P. Rodriguez, "Inertia emulation in AC/DC interconnected power systems using derivative technique considering frequency measurement effects," *IEEE Trans. Power Syst.*, vol. 32, no. 5, pp. 3338–3351, Sep. 2017.
- [31] S. Vachirasricirikul and I. Ngamroo, "Robust LFC in a smart grid with wind power penetration by coordinated V2G control and frequency controller," *IEEE Trans. Smart Grid*, vol. 5, no. 1, pp. 371–380, Jan. 2014.
- [32] J. Pahasa and I. Ngamroo, "PHEVs bidirectional charging/discharging and SoC control for microgrid frequency stabilization using multiple MPC," *IEEE Trans. Smart Grid*, vol. 6, no. 2, pp. 526–533, Mar. 2015.
- [33] H. Bevrani, *Robust Power System Frequency Control*, 2nd ed. New York, NY, USA: Springer, 2014.
- [34] H. Bevrani, F. Habibi, P. Babahajyani, M. Watanabe, and Y. Mitani, "Intelligent frequency control in an AC microgrid: Online PSO-based fuzzy tuning approach," *IEEE Trans. Smart Grid*, vol. 3, no. 4, pp. 1935–1944, Dec. 2012.
- [35] P. Kundur, *Power System Stability and Control*. New York, NY, USA: McGraw-Hill, 1994.
- [36] H. Bevrani, M. Watanabe, and Y. Mitani, *Power System Monitoring and Control*. Hoboken, NJ, USA: Wiley, 2014.
- [37] M. L. Chan, F. Scheweppe, and R. D. Dunlop, "Dynamic equivalents for average system frequency behavior following major disturbances," *IEEE Trans. Power App. Syst.*, vol. PAS-91, no. 4, pp. 1637–1642, Jul. 1972.
- [38] *Rate of Change of Frequency (ROCOF) Withstand Capability: ENTSO-E Guidance Document for National Implementation for Network Codes on Grid Connection*, European Network of Transmission System Operators for Electricity (ENTSO-E), Brussels, Belgium, 2017.
- [39] C. Wagner and H. Hagrass, "Toward general type-2 fuzzy logic systems based on zSlices," *IEEE Trans. Fuzzy Syst.*, vol. 18, no. 4, pp. 637–660, Aug. 2012.
- [40] R. Panel, "Stage one final determination: Review of the frequency operating standard," Austral. Energy Market Commission, Sydney, NSW, Australia, Tech. Rep. REL0065, 2017.



**THONGCHART KERDPOL** (S'14–M'16) received the B.Eng. and M. Eng. (Hons.) degrees in electrical engineering from Kasetsart University, Bangkok, Thailand, in 2010 and 2012, respectively. He received the Ph.D. degree in electrical and electronic engineering from the Kyushu Institute of Technology (Kyutech), Kitakyushu, Fukuoka, Japan, in 2016. From 2016 to 2017, he was a Post-Doctoral Fellow with the Department of Electrical and Electronic Engineering, Kyushu Institute of Technology, Japan. In 2018, he was a Visiting Researcher with the Institute of Electrical Power Engineering and Energy Systems (IEE), Clausthal University of Technology (TU Clausthal), Clausthal-Zellerfeld, Germany.

Since 2019, he has been a Senior Research Fellow with the Power System and Renewable Energy Laboratory (Mitani-Watanabe Lab), Kyushu Institute of Technology. Currently, he is developing a research project about inertia estimation of Japan power system using Phasor Measurement Units (PMU) with the Tokyo Electric Power Company (TEPCO), Japan. His research interests include power system stability, robust power system control, intelligent optimization, and smart/micro-grid control.



**MASAYUKI WATANABE** (S'03–M'05) received the B.Sc., M.Sc., and D. Eng. degrees in Electrical Engineering from Osaka University, Japan, in 2001, 2002, and 2004, respectively.

Since 2004, he has been with the Department of Electrical and Electronic Engineering, Kyushu Institute of Technology (Kyutech), Fukuoka, Japan, where he is currently working as an Associate Professor. He is the holder of the PMU licensed patent. He has authored books/book chapters, and over 100 journals/conference papers. He is also a member of the Institute of Electrical Engineers of Japan (IEEJ). His research interest includes the areas of the analysis of power systems.



**KOMSAN HONGESOMBUT** (S'99–M'03) received the B.Eng. and M. Eng. degrees in electrical engineering from the King Mongkut's Institute of Technology Ladkrabang (KMUTL), Bangkok, Thailand, in 1997 and 1999, respectively. He received the Ph.D. degree in electrical and electronic engineering from Osaka University, Osaka, Japan, in 2003. From 2003 to 2005, he was awarded a Postdoctoral Fellowship by Japan Society for the Promotion of Science (JSPS). As a

Postdoctoral Fellow, he worked on power system monitoring by application of GPS synchronized by PMU in the Department of Electrical Engineering at the Kyushu Institute of Technology, Japan. From 2005 to 2009, he was a specialist in power systems at the R&D Center of Tokyo Electric Power Company, Japan.

Since 2010, he has been with the Department of Electrical Engineering, Kasetsart University, Bangkok, Thailand, where he is currently working as an Assistant Professor. His research interests include the areas of the power system analysis and protection.



**YASUNORI MITANI** (M'87) received the Bachelor of Engineering, Master of Engineering, and Doctor of Engineering degrees from Osaka University, Osaka, Japan, in 1981, 1983 and 1986, respectively.

He is a Professor, the Director of Industry-Academic Collaboration Division and the Vice President of Kyushu Institute of Technology (Kyutech), Kitakyushu, Japan. From 1994 to 1995, he was a Visiting Research Associate with the University of California, Berkeley, USA. From 2016 to 2018, he served as the President for the Institute of Electrical Engineers of Japan (IEEJ), Power and Energy Society. He is a Distinguished Lecturer of the IEEJ, Power and Energy Society. He is also the holder of the PMU licensed patent. He has authored numerous books and book chapters, and over 250 journals and conference papers. His research interests include the areas of power system stability, dynamics, and control.

• • •